Asia-Pacific Journal of Science and Technology: Volume: 28. Issue: 06. Article ID.: APST-28-06-08. Research Article

APST

Asia-Pacific Journal of Science and Technology

https://www.tci-thaijo.org/index.php/APST/index

Published by the Research and Graduate Studies Division,
Khon Kaen University, Thailand

Effective field capacity prediction model for management of UAV spraying

Khemmapat Pucharoensilp[1], Khwantri Saengprachatanarug[1,2,*], Jetsada Posom[1,2], Seree Wongpichet[1], Kanda Saikeaw[1], Kittiphit Ungsathittavorn[3], Eizo Taira[4] and Sirorat Pilawut[5]

[1]Department of Agricultural Engineering, Faculty of Engineering, Khon Kaen University, Khon Kaen, Thailand
[2]Applied Engineering for Important Crops of the North East Research Group, Khon Kaen University, Khon Kaen, Thailand
[3]Pulsawattavorn Sugarcane Farm, Khon Kaen, Thailand
[4]Faculty of Agriculture, University of the Ryukyus, Okinawa, Japan
[5]Program of Agricultural Machinery Engineering, Faculty of Engineering, Rajamangala University of Technology ISAN Khonkaen Campus, Khon Kaen, Thailand
[*]Corresponding author: khwantri@kku.ac.th

Received 27 August 2022
Revised 3 November 2022
Accepted 12 November 2022

Abstract

The use of pesticides in agriculture is critical to maintaining the quality of agricultural production. Farmers are required to finish their spraying with high efficiency due to constraints in cost and time. Nevertheless, farmers need more knowledge and information required for managing Unmanned Aerial vehicles (UAV) spraying and providing the conditions of their fields because both data (management and field conditions) affect capacity. The field capacitance model was generated from UAV spraying (Tiger Drone) on a sugarcane field. Consequently, this research intended to discover the prediction model for effective field capacity for UAV spraying (Tiger Drone) in the sugarcane field. The procedure began by collecting the data of nine UAVs spraying in the sugarcane fields, for example, field, crop, UAV condition, and working times, to develop the prediction model for the UAV spraying in the sugarcane field. The prediction model was then validated using nine sugarcane fields collected correspondingly to the model's output. The conclusion presented was that the model's root mean square error (RMSE) was 0.14 m²/s. Farmers and providers can apply a predictive model to manage the spraying process and provide their field conditions.

Keywords: UAV, Sprayer, Effective field capacity, Predictive model, Management

1. Introduction

Many pests infest agricultural products and contribute to low yields [1]. Pesticides are recommended for controlling pests. Pest control must be completed in a short time because if these pests are not eliminated promptly, they can grow and become stronger. As a result, this can affect agricultural productivity and is hard to eliminate [2] if not controlled in time [3]. When the pest damage becomes more challenging to eliminate, farmers need to use more significant amounts of pesticide, which causes chemical residue and affects production costs. Weed population causes a 34% yield loss in arable crops worldwide [4]. Therefore, two million tons of pesticides are utilized annually worldwide, which is increasing rapidly. In 2020, global pesticide usage was estimated to increase by up to 3.5 million tons [5]. In order to avoid such problems, effective weed management planning is necessary.

Many countries have started using Unmanned Aerial vehicles (UAVs) in precision agriculture [6,7]. It is speedy and can reduce the workload of a farmer and the risk of exposure to dangerous chemicals during the spraying process [8]. UAVs are used with many agricultural plants, such as sugarcane [9], kale, onion, celery [10], paddy [11], cotton [12], olives, and citrus [13], which can get rid of weeds, protect plants from insects, and provide plants with medicine and fertilizer. However, the appropriate amount of time for spraying pesticide and herbicide is approximately 4-5 h, which can be applied during the low-temperature period of the day, such as the early morning or evening. Midday heat causes plant growth to slow down, and the herbicides quickly dry out on the

leaves, which reduces the amount of herbicide that the weeds absorb [14]. The timing of the first spraying of the season is, therefore, challenging because the proper spraying intervals are not continuous except at midday and are limited each day. If unable to spray on time in the season or in a manner suitable for eliminating weeds and insects, this problem will result in reduced production volumes. Farmers must work under exigency to finish spraying before pest growth and agricultural product damage. Poor spraying management causes increased spraying time, which is the main problem [15].

However, Thai farmers still need to gain the knowledge, information, and technology to manage the spraying process in their field conditions. Knowledge of time and UAVs' spraying capacity prior to spraying is essential. This information can be used to improve the management of UAV spraying, which will support planning and estimate the effective field capacity. This knowledge can then be used to prioritize spraying in his plot with the least amount of wasted time. The optimal spraying usually is in the morning and evening. Because it is the time when the stomata of the plant are open to allow the plant to absorb fertilizer or herbicide better, it will be the time when the calm wind ensures that the drone spray does not spread the mist to other areas. During the day, extreme heat closes the stomata and causes evaporation and a decrease in the number of chemicals. If they cannot spray at the right time, it will make the spraying of chemicals inefficient. The chemicals spread to other areas and include hazards for operators. All of them will result in farmers having more costs of using chemicals. Therefore, spraying at the right time is as crucial as spraying on time in each season. If not, older weeds or insects will grow too big. This model can help with the planning of spraying. On the same day, spraying will be completed promptly and work at full efficiency. At the right time of spraying (4-5 h) with the least wasted time for rework. When it can be planned to work well, there is no need to save much battery as well. During the midday, it is not suitable for spraying, and it will be able to recharge the battery for the next spraying period. Farmers can spray the chemicals at the planned time or at the right time to get rid of the weeds effectively if they have good estimation and management. This model will help farmers reduce costs and choose the right spraying interval for their fields. In addition, the contractor spraying chemicals with the hit will be able to plan the time of work and estimate the price of the notification more accurately. To the best of the author's observation, there are presently no articles about developing the effective field capacity (EFC) as a predictive device for UAV spraying in sugarcane fields.

For instance, various researchers who developed the spraying technique have studied a related topic. Koondee, et al. [16] studied the field capacity and variables of UAV operation time while spraying hormone fertilizer in a variable field plot design of a sugarcane field, and the results showed an average field capacity of 3.36 ha/hr and the longest plot could increase the working efficiency. The most time consumed was for the flight planning step [16]. Yousaf et al. [17] studied the field performance of the boom sprayer. The result indicated that for the same width of fields, the longer the field, the more productive time. Therefore, more will be the field efficiency of the sprayer. Because more time was required for turning at field ends due to less tractor maneuverability, the operator might have found difficulty controlling the tractor [17]. Wang et al. [18] conducted research to compare the droplet deposition, control efficacy, and working efficiency of a six-rotor UAV with a self-propelled boom sprayer and two conventional knapsack sprayers on the wheat crop. The working efficiency of the UAV was 4.11 ha/h, which was roughly 1.7-20.0 times higher than the three other sprayers [18]. Basso et al. [19] designed an embedded real-time UAV spraying control system supported by onboard image processing. The proposal used a normalized difference vegetation index (NDVI) algorithm to detect the exact locations where the chemicals are needed. The automated spraying control system used this information to perform punctual applications while the UAV navigated over the crops. This innovation reduces the cost of spraying chemicals because it uses fewer chemicals. Moreover, refilling the agrochemicals fewer times can reduce lost time and improve working efficiency [19]. Doungpueng et al. [8] developed an effective field capacity prediction model for selecting well-combined harvesters to field conditions. This research determines the prediction model from the conceptual model (physically-based and empirical models) by collecting data from 15 combined harvesters. The result showed that the RMSE of the model was 0.24 m^2/s [8]. This apprehension can be used to select the appropriately combined harvesters, plan the harvest, and estimate the effective field capacity. So, this research has the creative concept of combining the prediction model with the physically-based model and the empirical model for the accuracy of field conditions. In other words, farmers and providers can choose to use the proper UAV for their plots. It will help plan for spraying and estimate the effective field capacity.

These studies developed the UAV spraying technology and increased its performance. The UAV spraying can work quickly with high performance. In order to use drones for spraying in a large area, it is crucial to have proper management for the best performance. Proper management is essential to improving drone performance because the working time can be predicted precisely based on each field condition. Moreover, proper management can increase the performance of the battery's usage. This reduces the time to charge the battery and the time of transportation and can precisely calculate the fair cost for the customers, resulting in a reduction in the cost of a sprayed operation. Hence, there has to be a study about the active and passive working times at every step. The area, field shape, field length, and UAVs' condition can affect the working time [16], such as when creating the flight mission time, chemical mixing time, headland turning time, field boundary spraying time, traveling time, battery changing time and chemical filling and spraying time. If drone users have an equation model to predict

the effective field capacity, there can be an increase in service performance. However, there needs to be research about the function of the estimated time in each crop field or the method for predicting the precise usage time.

Hence, the model will provide helpful guidance for the user in planning spraying management. It benefits the user through shorter spraying time and reduces the time lost in the spraying process. It can also be adapted into an application for agriculture management. Thus, the main contributions of this paper aim to;

• Develop an effective field capacity model for predicting the field capacity of UAV spraying in the sugarcane field.
• Evaluate the effective field capacity prediction model's performance.
• Determine the lost time of the UAV spraying to develop a method to reduce the lost time.

2. Materials and methods

The working procedure (Figure. 1) began by collecting the log data of nine service UAVs spraying in the sugarcane fields, such as field, crop, UAV condition, and working times, to develop the UAV spraying prediction model in the sugarcane field. The model was then validated using log data from nine service UAVs spraying in sugarcane fields corresponding to the model's creation.

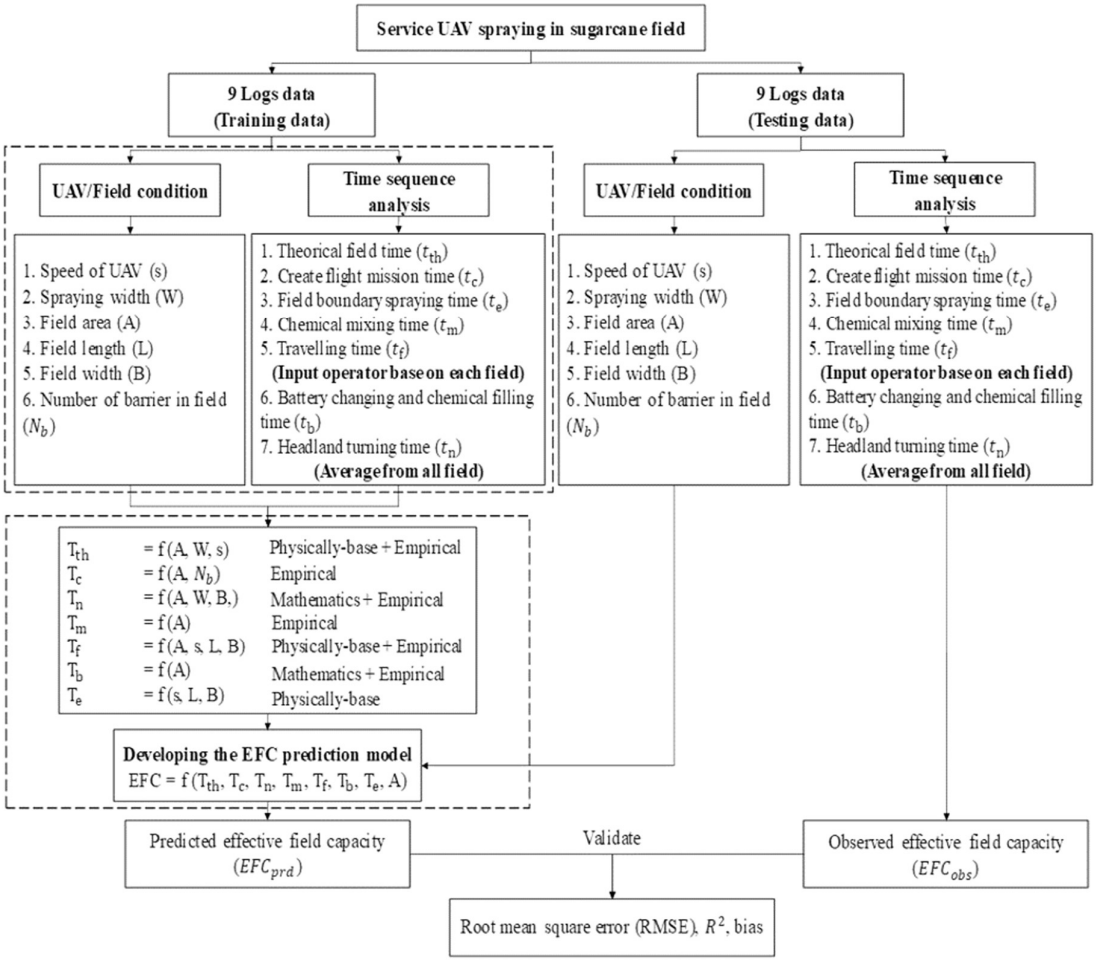

Figure 1 Working procedure in this research.

2.1 Instrument

Field size and field shape can affect the EFC of the UAV spraying [16]. This research assumes that most sugarcane fields are rectangular. Log data was selected from the service of a UAV spraying in a sugarcane field in Thailand. Spraying weed management in the sugarcane field was operated from the field preparation before growing sugarcane to harvesting in 2020. The multi-rotor UAV sprayer (Tiger Drone, HG Robotic Thailand) was selected in this study.

2.2 Theory of EFC

There are two types of field capacities for UAV spraying: theoretical field capacity (TFC) and EFC. The equations for field capacities are presented in Equations (1) and (2), respectively.

$$\mathrm{TFC} = \frac{\mathrm{A_{total}}}{\mathrm{T_{th}}} \tag{1}$$

$$\mathrm{EFC} = \frac{\mathrm{A_{total}}}{\mathrm{T_{total}}} \tag{2}$$

where $\mathrm{A_{total}}$ is the total spraying area ($\mathrm{m^2}$), $\mathrm{T_{th}}$ is the theoretical spraying field hour (s), and $\mathrm{T_{total}}$ is the total spraying hour (s).

The TFC can be determined from UAV spraying without any loss of time from the running time [20]. Nevertheless, in practice, there is no downtime-free UAV spraying because several factors affect the UAVs behavior during spraying, including crop height, field conditions, and the UAV itself. These factors cause downtimes and are reconciled with $\mathrm{T_{th}}$ to $\mathrm{T_{total}}$. All working times are shown in the flow chart in Figure 2.

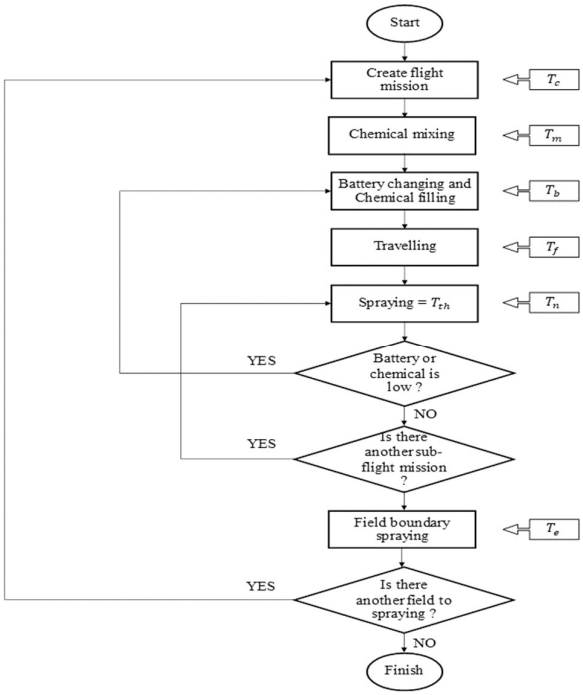

Figure 2 UAV spraying processes in practical fields.

The activities while the UAV spraying is running in the field (passive working and active working) are labeled "total lost time" (TL). This TL is set apart into the flight mission creation time ($\mathrm{T_c}$), the chemical mixing and preparation time before the flight mission starts ($\mathrm{T_m}$), the headlands turning time ($\mathrm{T_n}$), the traveling for battery changing and chemical filling time ($\mathrm{T_f}$), and the battery changing and chemical filling time when the sub-flight mission is finished ($\mathrm{T_b}$). Moreover, the remote pilot does not create flight missions until the field's borders because the trees are used for rest during hard work. The UAV spraying loses time for field boundaries by manual flight, called field boundary spraying lost time ($\mathrm{T_e}$). Ultimately, the EFC can be obtained from Equation (3).

$$\mathrm{EFC} = \frac{\mathrm{A_{total}}}{\mathrm{T_{th}+TL}} = \frac{\mathrm{A_{total}}}{\mathrm{T_{th}+(T_c+T_m+T_n+T_f+T_b+T_e)}} \tag{3}$$

2.3 Improvement of the predictive model for EFC

The elementary predictive model for the EFC is presented in Equation (3). Nonetheless, differences in the physical characteristics of each UAV spraying can affect EFC. Therefore, the Tiger Drone was selected for this study. The research began by collecting information, including field, crop, and spraying conditions from nine

randomly chosen sugarcane fields in 2020 for use in developing the prediction model. This research has the creative concept of combining the prediction model with the physically-based and empirical models. This study makes the equations accurate and changes according to field conditions. The physically-based model analyzes physical theories such as the velocity equation (v=s/t) and geometric equations. Empirical models are constructed by correlating variables from actual performance in each field condition to improve the model. The selected sample data (9 sugarcane fields) is a feasibility study of this model.

The time parameters of the actualization (T_{th}, T_c, T_m, T_n, T_b, T_f, and T_e) work in the field for spraying herbicides or fertilizers, as shown in Figure 3. They were found by log data in the UAVs. The first flight of a UAV without spraying in the field creates flight mission time and gap time. After the first flight and starting the second flight, the chemical mixing time starts. When the UAV opens, the nozzle pump is the theoretical time, and the UAV closed nozzle pump is turning the headland time. The working of the battery changing and then the chemical filling time are the time that finishes the spraying flight for landing. During sub-flight missions, the gap time is the battery changing and the chemical filling time.

Furthermore, the field boundary spraying time has been after a flight mission without a planning path. All data and time parameters are used in the calculation of the relative equation and coefficient, for example, k_s, k_a, k_b, k_m, and k_{nf}, by simple linear regression and multilinear regression (MLR) analysis. Eventually, the prediction model of the EFC for the Tiger Drone UAVs is shown in Equation (22).

2.3.1 Improvement of the predictive model for the theoretical spraying field time (T_{th})

If a UAV spraying has an actual spraying speed (S_s) same as its setting spraying speed (S) and sprays with a constant sprayer width (W), then the spraying is done without TL. The TFC and T_{th} can be obtained from Equations (4) and (5), respectively [21,22]. Nevertheless, the actual spraying speed is not constant and is not equal to the set speed because UAVs need to accelerate from the starting position (start flight mission and turning), and the wind also affects the spraying speed.

$$TFC = W \times S = \frac{A_{total}}{T_{th}} \tag{4}$$

$$T_{th} = \frac{A_{total}}{W \times (Sk_s + z)} \tag{5}$$

where W is the sprayer width (m), S is the setting spraying speed (m/s), k_s is the amount of spraying speed, and z is the intercept.

2.3.2 Improvement of the predictive model for the create flight mission time (T_c)

To create a flight mission, the remote pilot will visually assess the overall plot and use manual drones to explore the plot while also marking the edge of the plot and the risk points that may harm the spraying drones (trees, poles). Create flight mission time is related to the area and obstacle. Therefore, T_c can be solved via Equation (6).

$$T_c = A_{total}k_a + N_B k_b + c \tag{6}$$

where N_B is the number of barriers in the field, k_a is the coefficient of the area, k_b is the coefficient of the number of barriers in the field, and c is the intercept.

2.3.3 Improvement of the predictive model for the chemical mixing time (T_m)

Most of the chemicals can be used for spraying after they are mixed with water or specific chemicals, and they can then be used for spraying plants. As such, there is a mixing process before spraying. Typically, the volume of the water and the chemicals have a relationship with the area (A_{total}), and the chemical mixing time has a relationship with the volume of water and chemicals [16], which causes the chemical mixing lost time (T_m) to have a relationship with the area, as shown in Equation (7).

$$T_m = A_{total}k_m + d \tag{7}$$

where k_m is the coefficient of the chemical mixing time, and d is the intercept.

2.3.4 Improvement of the predictive model for the headland turning time (T_n)

Normally, the remote pilot will create spraying path plans that spray along a longitudinal path of the field. Due to the least number of headlands turning, it will reduce the lost time. Therefore, this section describes the development of a loss time prediction model during headland turning.

The UAV spraying works with the UAV at the starting point (camp, take-off, and landing point). Following this, the UAV travels to the starting mission point. Next, it travels and sprays until its headlands. After that, the UAV stops spraying and turns to the next row. Thus, the number of field rows equals the number of headlands turning. Then, the number of headlands turning (N_t) can be calculated as Equation (8). When the UAV has reached the last point of a sub-flight mission, it will not turn back but will continue traveling to the camp. Consequently, the sub-flight mission will not have headlands turning in the last row. Thus, it is vital to know the number of sub-flight missions (N_f). Usually, the remote pilot will create a sub-flight mission with an area of 4800 m², which is normally appropriate for the battery capacity and the container's volume of the Tiger Drone. When there is a wind flow or the wind direction is not appropriate, it may change the plan of the UAV spraying, which can result in an improper N_f. Thus, the coefficient of k_{nf} was used to adjust the N_f with greater accuracy, as found in Equation (9). When using N_t combined with the turning time, it will be headland turning lost time (T_n), as found in Equation (10). The coefficient of the number of sub-flight missions (k_{nf}) if the field is a non-rectangle (rectangle, k_{nf}= 1) is in Equation (11).

$$N_t = \frac{B}{W} \tag{8}$$

$$N_f = \frac{A_{total}}{4800 \times k_{nf}} \tag{9}$$

$$T_n = t_{nt} \times \left(\frac{B}{W} - \frac{A_{total}}{4800 \times k_{nf}}\right) \tag{10}$$

$$k_{nf} = \frac{A_{total}}{4800 \times N_f} \tag{11}$$

where B is the field width (m), W is the sprayer width (m), t_{nt} is the time of the headland turning once times (s), and k_{nf} is the coefficient of the number of sub-flight missions.

2.3.5 Improvement of the predictive model for battery changing and chemical filling time (T_b)

Before starting each sub-flight mission, one must change the battery and fill the chemical for every mission. Therefore, the number of battery changes and chemical fills will equal the number of sub-flight missions found in equation (9). However, there has to be more than one times to it, because after finishing the flight mission, there will be spraying for the field boundary of the area with one flight. The battery changing and chemical filling lost time (T_b) can be found in Equation (12).

$$T_b = t_{bt} \times \left(\frac{A_{total}}{4800 \times k_{nf}} + 1\right) \tag{12}$$

where t_{bt} is the time of battery changing and chemical filling once (s).

2.3.6 Improvement of the predictive model for traveling to field time (T_f)

When UAVs have a depleted battery or a chemical or finish a sub-flight mission in the field, they cannot continue to spray and need battery changing and chemical filling first. Mileage is not specified and revolves around the tank's capacity. Therefore, the approximate distance traveled can be determined by applying the average length between the field hub and the camp (the launch and landing points) (L_{tra}), given in Equation (13). T_f can be determined by the proportion of all lengths that remain between the distance traveled from the hub of the field to the camp (L_{tra}) and the velocity of travel for battery changing and chemical filling (S_f), shown in Equation (14). However, there are two round-trip flights at every start and end of a sub-flight mission, so the number of sub-flight missions combined with traveling speed and distances are calculated as T_f in Equation (15).

$$L_{tra} = \sqrt{\frac{L_{avg}}{2}^2 + \frac{B}{2}^2} \tag{13}$$

$$T_f = \frac{1}{Sf} \times \sqrt{\frac{L_{avg}}{2}^2 + \frac{B^2}{2}} \quad (14)$$

$$T_f = \frac{2}{S_f} \times \sqrt{\frac{L_{avg}}{2}^2 + \frac{B^2}{2}} \times \left(\frac{A}{4800 \times k_{nf}} + 1\right) \quad (15)$$

where L_{avg} is the average field length (m), B is the field width (m), and S_f is the traveling speed for battery changing and chemical filling (m/s).

2.3.7 Improvement of the predictive model for field boundary spraying time (T_e)

Field boundary spraying is used in at-risk areas that can damage the drone or in areas that are not on the spraying plan. The manual control by the remote pilot at every site after finishing the spraying follows the spraying plan. Normally, there will be a field boundary spraying process. Then, one has to calculate the length of the area's circumference (L_{cir}), found in Equation (16). However, a sugarcane field can be something other than a rectangular area, as always: it may not be a symmetrical area or even have a concave one. Thus, the spraying speed of field boundary spraying used to adjust the T_e for greater accuracy can be found in Equation (17).

$$L_{cir} = 2 \times (L_{avg} + B) \quad (16)$$

$$T_e = \frac{2 \times (L_{avg} + B)}{S_e} \quad (17)$$

where S_e is the spraying speed for field boundary spraying (m/s).

2.3.8 Elementary predictive model of the EFC for the Tiger Drone

By conjugating all the predictive models of T_{th}, T_c, T_m, T_n, T_b, T_f, and T_e, the elementary predictive model for the EFC of the UAV spraying is shown in Equation (18).

$$EFC = \frac{A_{total}}{\left(\frac{A_{total}}{W \times (Sk_S + z)}\right) + (A_{total}k_a + N_B k_b + c) + (A_{total}k_m + d) + \left(t_{nt} \times \left(\frac{B}{W} - \frac{A_{total}}{4800 \times k_{nf}}\right)\right)} \Bigg/ \left(t_{bt} \times \left(\frac{A_{total}}{4800 \times k_{nf}} + 1\right)\right) + \left(\frac{2}{Sf} \times \sqrt{\frac{L_{avg}}{2}^2 + \frac{B^2}{2}} \times \left(\frac{A_{total}}{4800 \times k_{nf}} + 1\right)\right) + \left(\frac{2 \times (Lavg + B)}{Se}\right) \quad (18)$$

2.4 Validation of the predictive model for the sugarcane

Confirmation of the model mentioned above should be rehearsed to validate and appraise the model. First, the information from nine sugarcane fields in October 2020 (different location and time of training data) were collected. The root mean square error (RMSE) is a method used to expedient the contrast in the EFC between predicted and observed EFC [23], as given in Equation (19) underneath:

$$RMSE = \sqrt{\frac{\sum (EFC_{obs} - EFC_{prd})^2}{n}} \quad (19)$$

where EFC_{obs} is the observed EFC (m^2/s), EFC_{prd} is the predicted EFC (m^2/s), n is the total number of spraying fields.

The R^2 presents the ratio of the deviation in the independent variable that can be elucidated by the deviation in the surveyed information, as presented in Equation (20).

$$R^2 = 1 - \frac{\sum (EFC_{obs} - EFC_{prd})^2}{\sum (EFC_{obs} - \overline{EFC}_{obs})^2} \quad (20)$$

where $\overline{EFC}_{obs}$ is the mean of the measured values (observed data).

The bias, which is the average divergence between the surveyed information and the information predicted by the EFC model and represents the overall accuracy of the calibration Equation, is given by Equation (21).

$$\text{bias} = \frac{\sum(\text{EFC}_{\text{obs}} - \text{EFC}_{\text{prd}})^2}{\text{n}} \quad (21)$$

3. Results and discussion

3.1 Improvement of the predictive model for EFC

Equation (3) presents the equation for the EFC formula, including A_{total}, T_{th}, and the six lost times (T_c, T_m, T_n, T_f, T_b, and T_e). This section presents methods developed for a predictive model for T_{th}, T_c, T_m, T_n, T_f, T_b, and T_e will be conveyed in this part. Table 1 exposes field and UAV condition data collected from the nine sugarcane fields. The averages of the field parameters (Field total area (A_{total}), Field Width (B), Field average length (L_{avg}), and the Number of barriers in the field (N_b) are 8,826 m^2, 62.9 m, 142.1 m, and 0.44 points, respectively. Moreover, the averages of the UAV parameters (Working width (W), Setting spraying speed (S), Actual spraying speed (Ss), Time of headland turning once times (t_{nt}), Time of battery changing, and Chemical filling once times (t_{bt}), Traveling speed (S_f), Spraying speed for field boundary spraying (S_e), and the Number of sub-flight missions (N_f)) are 4.00 m, 3.67 m/s, 2.90 m/s, 5.93 s, 162.2 s, 1.95 m/s, 2.34 m/s, and 2.2 flights, respectively. Table 2 exposes the observed data for sugarcane fields. The T_{th} and lost time through spraying (T_c, T_m, T_n, T_n, T_f, and T_e) expose that the average T_{th} was 624.6 s, and the averages of T_c, T_m, T_n, T_n, T_f, and T_e were 385.0 s, 719.4 s, 134.5 s, 402.3 s, 267.1 s, and 179.6 s, respectively. Thus, the calculation from the relative of an actual spraying speed and setting spraying speed is in Figure 3. The coefficient and intercept of k_s and z are 0.65 and 0.51 from Figure 3, used to adjust the T_{th} for better accuracy. Create flight mission time is related to the area and obstacle, as shown in Figure 4. When correlated with maximum residue limits (MRL), the coefficient and intercept of k_a, k_b, and c are 0.005, 278.2, and 214.9, respectively. Which causes the chemical mixing lost time (T_m) to have a relationship with the area (Figure 5). From Figure 5, the coefficient and intercept of k_m and d are .0 and -10.65, respectively. The coefficients of k_{nf} were 0.72 (if the field shape is a non-rectangle) and t_{nt} was 5.93 s, calculated using the area N_f and t_{nt} in Table 1. In summary, the predictive model of the effective field capacity of UAVs while spraying the sugarcane fields is given by Equation (22).

Table 1 Parameters of field and conditions of UAV for the advancement of the elementary predictive model.

No.	Field					UAV							
	A (m^2)	B (m)	L_{avg} (m)	N_b	Shape	W (m)	S (m/s)	Ss (m/s)	t_{nt} (s)	t_{bt} (s)	S_f (m/s)	S_e (m/s)	N_f
P1	4,203	48.6	83.3	0	Rec.	4	3	2.51	3.74	105.2	1.00	1.53	1
P2	4,663	57.5	81.2	0	Rec.	4	3	2.66	4.09	108.8	1.51	1.83	1
P3	10,583	71.4	148.2	1	Rec.	4	4	2.93	5.76	270.3	2.53	1.57	2
P4	9,861	35.9	274.6	0	Rec.	4	4	3.35	8.30	121.5	2.30	2.46	2
P5	17,377	103.5	173.8	0	Non-rec	4	4	3.08	5.19	145.7	2.94	3.39	5
P6	7,076	52.8	134.1	0	Rec.	4	4	2.80	5.12	152.1	1.76	2.57	2
P7	7,815	59.1	132.5	1	Rec.	4	5	3.94	7.69	124.0	1.99	3.15	2
P8	4,684	61.7	75.9	0	Rec.	4	3	2.38	5.99	149.9	1.59	1.87	2
P9	13,176	75.2	175.3	2	Rec.	4	3	2.49	7.45	282.5	1.97	2.73	3
Avg	8,826	62.9	142.1	0.44		4.0	3.67	2.90	5.93	162.2	1.95	2.34	2.2

Table 2 Observed working times for the advancement of the elementary predictive model.

No.	T_{th} (s)	T_c (s)	T_m (s)	T_n (s)	T_b (s)	T_f (s)	T_e (s)
P1	413.8	278.0	224.7	59.8	315.7	167.1	159.5
P2	406.9	181.9	492.5	45.0	217.6	229.7	163.5
P3	676.1	507.2	746.0	198.5	540.6	382.8	150.5
P4	554.9	234.7	731.0	91.3	242.9	92.9	147.7
P5	1,135.0	320.1	1,381.0	212.1	728.4	413.2	221.0
P6	538.0	247.0	677.4	133.1	304.2	183.2	170.0
P7	449.7	453.0	633.0	174.0	124.0	257.8	223.0
P8	569.2	341.1	348.1	126.1	299.9	242.2	161.7
P9	877.7	902.0	1,240.7	170.8	847.6	435.1	219.7
Avg	624.6	385.0	719.4	134.5	402.3	267.1	179.6

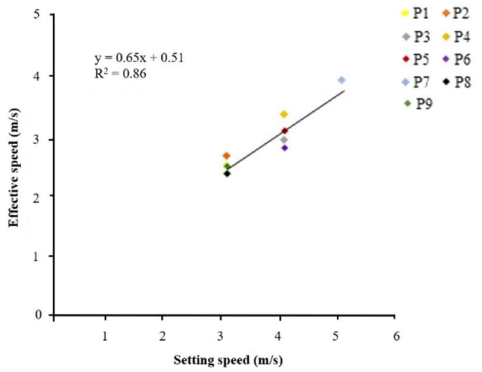

Figure 3 Relationship of the setting speed and effective speed for T_{th}.

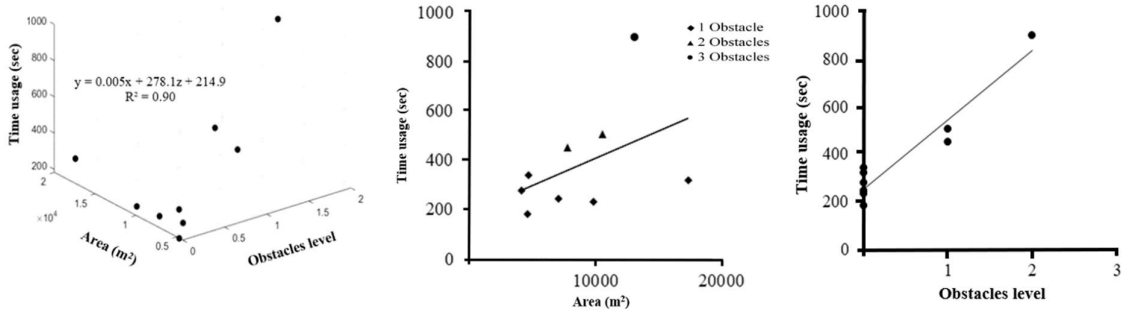

Figure 4 Relationship of the create flight mission time, Area and Obstacle level for T_c.

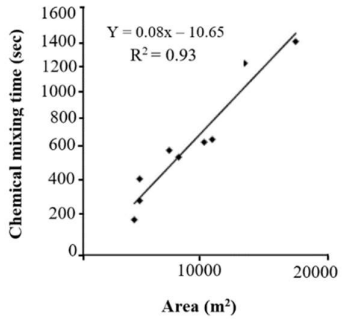

Figure 5 Relationship of the area and chemical mixing time for T_m.

$$EFC = \frac{A_{total}}{\left(\frac{A_{total}}{W\times(0.6522S\quad .5132)}\right)+(0.0053A_{total}+278.1869N_B+214.9750)+(0.0827\quad _{total}-10.651)} \quad (22)$$
$$\left(5.93\times\left(\frac{B}{W}-\frac{A_{total}}{4800\times 1}\right)\right)+\left(162.23\times\left(\frac{A_{total}}{4800\times 1}+1\right)\right)+\left(\frac{2}{Sf}\times\sqrt{\frac{L_{avg}{}^2}{2}+\frac{B^2}{2}}\times\left(\frac{A_{total}}{4800\times 1}+1\right)\right)+\left(\frac{2\times(L_{avg}+B)}{Se}\right)$$

Figure 6 shows the working time analysis of the nine sugarcane fields used to develop the prediction model. The UAV spraying spent sequentially 23% and 77% of its time for T_{th} and TL. Nevertheless, the EFC of the UAV spraying reduces due to the response of the TL. The TL was synthesized by six loss times (T_c, T_m, T_n, T_b, T_f, and T_e). The TL can be divided into two types: the major effects of lost time and the minor effects of lost time. The T_m and T_b formed a main-effect group, contributing 27% and 18% of the lost time, individually, and therefore have a large impact on the EFC. These lost times were affected by worker experiences and chemical properties. On the other hand, the proportions of the less effective group were T_c, T_n, T_f, and T_e, which were discretely 13%, 3%, 10%, and 6% of the lost time. These lost times were determined by field conditions, such as the shape of the field and the number of obstacles [16]. However, they did not have a strong effect on the EFC. Finally, further study should focus on reducing lost time, for example, T_m and T_b can be decreased by the chemical mixer machine and developing the new battery. If it takes time to mix chemicals faster than people can discharge them into the

drone tank with an automatic system, the new battery can be replaced more easily. So, it will reduce the lost time. Additionally, the model performance of other UAVs and plant cultivars should be investigated.

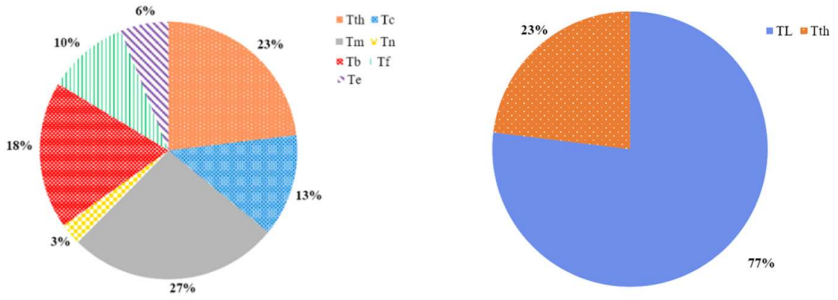

Figure 6 Working times of the 9 sugarcanes field used to develop a predictive model.

3.2 Validation of the predictive model of EFC for UAV spraying

Table 3 presents data on field and UAV conditions from the nine sugarcane fields in October 2020, and Table 4 presents observed and predicted operational times. The TFC (existing method) was calculated accepting Equation (1), and the observed EFC of the nine UAVs spraying in the sugarcane fields (EFC_{obs}) was determined by applying Equation (3); the results are presented in Table 4. The range of EFC_{obs} 2.71 m^2/s to 3.70 m^2/s. Moreover, the parameters in Table 3 were inserted in Equation (22) and used to find EFC_{prd}, as presented in Table 4. The EFC_{prd} ranged from 2.40 m^2/s to 3.61 m^2/s. Eventually, the EFC_{prd} and the EFC_{obs} were validated with an RMSE of 0.14 m^2/s, an R^2 of 0.91, and a bias of 0.02 m^2/s, as presented in Figure 7.

Table 3 Parameters of field and conditions of UAV for validation of the predictive model.

No.	Field conditions					UAV							
	A (m^2)	B (m)	L_{avg} (m)	N_b	Shape	W (m)	S (m/s)	S_s (m/s)	t_{nt} (s)	t_{bt} (s)	S_f (m/s)	S_e (m/s)	N_f
V1	13,321	83.6	159.4	1	Rec.	4	3	2.61	4.34	142.9	1.01	2.74	6
V2	7,301	42.5	173.1	0	Rec.	4	4	2.93	4.19	217.9	1.30	2.68	2
V3	6,015	43.2	136.8	1	Non-rec.	4	3	2.45	4.43	281.9	0.62	2.55	3
V4	19,356	79.1	247.1	0	Rec.	4	4	3.43	4.27	184.2	1.38	3.25	4
V5	11,722	101.0	115.0	0	Rec.	4	4	3.08	4.41	207.3	0.83	2.24	3
V6	6,440	56.7	122.4	0	Rec.	4	5	3.99	4.04	384.4	1.62	3.35	2
V7	6,508	60.6	113.9	0	Rec.	4	4	3.16	4.94	249.7	1.56	4.15	2
V8	4,977	52.1	98.9	0	Rec.	4	4	3.05	4.96	263.8	1.24	1.98	2
V9	8,413	53.1	164.8	0	Rec.	4	4	3.12	4.23	204.4	1.49	2.56	3
Avg	9,339	63.54	147.9	0.22		4	3.89	3.09	4.42	237.4	1.23	2.83	3.00

Table 4 Observed and predicted working times for the validation of the predictive model.

No.		T_{th} (s)	T_c (s)	T_m (s)	T_n (s)	T_b (s)	T_f (s)	T_e (s)	EFC (m^2/s)	TFC (m^2/s)
V1	Observed	1,263.5	833.5	1,147.7	104.1	857.1	550.8	159.7	2.71	12.00
	Predicted	1,348.4	563.8	1,091.0	112.1	787.6	527.9	177.3	2.89	
V2	Observed	469.2	267.5	537.9	58.4	435.8	309.8	232.0	3.16	16.00
	Predicted	584.6	253.7	593.2	53.9	409.0	271.5	160.9	3.14	
V3	Observed	662.9	467.9	419.7	62.0	845.8	186.7	215.4	2.10	12.00
	Predicted	608.9	525.0	486.8	58.7	444.6	237.6	141.2	2.40	
V4	Observed	1,288.6	285.1	2,049.6	92.6	736.8	493.9	290.4	3.70	16.00
	Predicted	1,550.0	317.6	1,590.2	93.3	816.5	789.1	200.7	3.61	
V5	Observed	730.0	358.4	881.3	83.7	622.0	500.3	214.8	3.46	16.00
	Predicted	938.7	277.1	958.8	135.3	558.4	318.4	192.9	3.47	
V6	Observed	352.5	294.1	597.2	76.8	384.4	93.2	145.3	3.31	20.00
	Predicted	426.6	249.1	522.0	76.1	379.9	190.9	106.9	3.30	
V7	Observed	549.3	285.6	674.3	59.3	249.7	52.8	81.5	3.33	16.00
	Predicted	521.1	249.5	527.6	81.8	382.2	183.7	84.1	3.21	
V8	Observed	389.9	305.5	378.8	124.1	263.8	270.1	95.2	2.72	16.00
	Predicted	398.6	241.4	401.0	71.1	330.4	137.6	152.5	2.87	
V9	Observed	537.0	379.8	487.5	75.4	613.1	327.9	204.4	3.20	16.00
	Predicted	673.7	259.6	685.1	68.3	446.6	288.0	170.2	3.25	
S.D.	Observed	351.0	179.2	528.5	22.1	234.0	179.7	67.5	0.48	2.40
	Predicted	411.9	126.1	385.0	26.3	179.3	206.6	38.4	0.36	

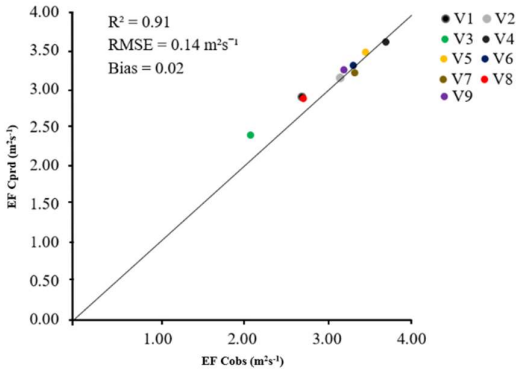

Figure 7 Relationship of the observed and predicted effective field capacity.

4. Conclusion

Farmers and providers could use the effective field capacity prediction model for estimating their UAV field capacity. This model was flexible to change the average and coefficient to CO-insigne for use with other converters or drones, such as W, Ss, t_{bt}. Users of the equation would be able to modify these parameters for future use with their plots and drones.

The model predicting effective field capacity was validated using nine sugarcane fields; therefore, it was validated using nine UAVs spraying in the sugarcane field to confirm the predictive accuracy. Finally, the results presented the RMSE between the observed and the predicted EFC; the RMSE was 0.14 m^2/s i.e., nearly zero, indicating that the referred prediction model for the UAV spraying in the sugarcane field could be used to estimate effective field capacity. By using this model, the field conditions can control the spraying process to shorten the spraying time and reach production capacity.

Finally, further study should focus on developing an effective field capacity prediction model and reducing lost time. Future research may explore the relationship between tank capacity, area, and flow rate as a function to represent this number so that the EFC model can be used with varying drone sizes. Moreover, the design of the automatic agrochemical mixer will reduce the major lost time.

5. Acknowledgments

The author thanks the North East Thailand Cane and Sugar Research Center (NECS) and the Research and Graduate Studies, Khon Kaen University for funding this research. Additional thanks to the HG Robotic Company (Thailand) and the Bindee Agritech Company (Thailand) for sponsoring the drone and to Mr. Kittiphit Ungsathittavorn for providing the experimental field.

6. References

[1] Dormon AH, Leeuwis C. Effectiveness and profitability of integrated pest management for improving yield on smallholder cocoa farms in Ghana. Int J Trop Insect Sci. 2007;27(1):27-39.

[2] Srivastava T, Singh A, Srivastava S. Critical period of crop-weed competition in sugarcane ratoon. Indian J Weed Sci. 2002;34(3 and 4):320-321.

[3] Sudhiarom S. Study and improvement on the efficacy of pest control [Internet]. 2016 [cited 2021 Feb 27]. Available from: https://www.doa.go.th/research/attachment.php?aid=2206.

[4] Oerke EC. Crop losses to pests. J Agric Sci. 2006;144(1):31-43.

[5] Sharma A, Kumar A, Shahzad B, Tanveer M, Sidhu GPS, Handa N, et al. Worldwide pesticide usage and its impacts on ecosystem. SN Appl Sci. 2019;1(11):1446.

[6] Zhang C, Kovacs JM. The application of small unmanned aerial systems for precision agriculture: a review. Precis Agric. 2012;13(6):693-712.

[7] Kulkarni SC, Natu AS. Adoption and utilization of drones for advanced precision farming: a review. Int J Recent Innov Trends Comput Commun. 2016;4(5):563-565.

[8] Doungpueng K, Saengprachatanarug K, Posom J, Chuan-Udom S. Selection of proper combine harvesters to field conditions by an effective field capacity prediction model. Int J Agric Biol Eng. 2020;13(4):125-134.

[9] Mogili UR, Deepak BBVL. Review on application of drone systems in precision agriculture. Procedia Computer Sci. 2018;133:502-509.

[10] Zhang XQ, Song XP, Qin ZQ, Zhang BQ, Wei JJ, Li YR, et al. Effect of spray parameters of drone on the droplet deposition in sugarcane canopy. Sugar Tech. 2020;22(2):583-588.
[11] Opanukul W, Saicomfu A, Pinyawattoe P, Tiantad I, Thongdang B, Sukprasert V, editors. Drone research for organic agriculture. Proceeding of the 18th TSAE national Conference; 2017 Sep 7; Bangkok, Thailand. 2017.
[12] Punyawattoe P, Worawit S, Chaiyasing N, Supornsin S. The efficacy of the unmanned aerial vehicle (UAV) for controlling rice dirty panicle disease. Thai Agric Res J. 2019;37(1):27-36.
[13] Lou Z, Xin F, Han X, Lan Y, Duan T, Fu W. Effect of unmanned aerial vehicle flight height on droplet distribution, drift and control of cotton aphids and spider mites. Agronomy. 2018;8(9):187.
[14] Martinez-Guanter J, Agüera P, Agüera J, Pérez-Ruiz M. Spray and economics assessment of a UAV-based-ultra-low-volume application in olive and citrus orchards. Precis Agric. 2019;21(1):226-243.
[15] Stack L, editors. New England greenhouse floriculture guide; a management guide for insects, diseases, weeds and growth regulators. Northeast Greenhouse Conference; 2010 Nov 3-4, Worcester, United States. Massachusetts: University of Massachusetts Amherst; 2010.
[16] Koondee P, Saengprachathanarug K, Posom J, Watyotha C, Wongphati M. Study of field capacity and variables of UAV operation time during spraying hormone fertilizer in sugarcane field. Earth Environ Sci. 2019;301:012020.
[17] Yousaf K, Iqbal M, Iqbal T, Hanif M. Effect of field plot design on the efficacy of boom sprayer. Univers J Agric Res. 2014;2(7):236-241.
[18] Wang G, Lan Y, Yuan H, Qi H, Chen P, Ouyang F, et al. Comparison of spray deposition, control efficacy on wheat aphids and working efficiency in the wheat field of the unmanned aerial vehicle with boom sprayer and two conventional knapsack sprayers. Appl Sci. 2019;9(2):218.
[19] Basso M, Stocchero D, Ventura Bayan Henriques R, Vian AL, Bredemeier C, Konzen AA, et al. Proposal for an embedded system architecture using a GNDVI algorithm to support UAV-based agrochemical spraying. Sensors. 2019;19:5397.
[20] Hunt D. Farm power and machinery management. 9th ed. Iowa, ISU press; 1995.
[21] American Society of Agricultural and Biological Engineers (ASABE) [Internet]. Michigan: The Association; c1907-2021 [cited 2021 May 18]. ASABE standards published. Available from: https://www.asabe.org/PublicationsStandards/StandardsDevelopment/NationalStandards/Published-Standards.
[22] Chuan-Udom S. Grain harvesting machines. 1st ed. Khon Kaen: Khon Kaen University Press; 2013.
[23] Mostafa KM, Quazi KH, Ehsan HC. Development of a remote sensing-based rice yield forecasting model. Span J Agric Res. 2016;14(3):1-11.